Available on the CERN CDS information server **CMS PAS HIG-11-029**

CMS Physics Analysis Summary

Contact: cms-pag-conveners-higgs@cern.ch 2011/12/13

Search for Neutral Higgs Bosons Decaying to Tau Pairs in pp Collisions at $\sqrt{s} = 7$ TeV

The CMS Collaboration

Abstract

A search for neutral Higgs bosons in proton-proton collisions at the LHC at a center-of-mass energy of 7 TeV is presented. The results are based on a data sample corresponding to an integrated luminosity of 4.6 fb^{-1} recorded by the CMS experiment. The search uses decays of the Higgs bosons to tau pairs, including the cases where the Higgs boson is produced in association with a b-quark jet (MSSM search) or two forward jets from vector boson fusion Higgs boson production (SM search), or where the tau pair has large transverse momentum (SM search). No excess is observed in the tau-pair invariant-mass spectrum. The resulting upper limits on the Higgs boson production cross section times branching fraction to tau pairs, as a function of the pseudoscalar Higgs boson mass, yield stringent new bounds in the MSSM parameter space, excluding values of $\tan\beta$ as low as 7.8 at a m_A =160 GeV. In the SM case, the data exclude at 95% CL a Higgs boson with a production cross section between 2.8 and 6.3 times that in the standard model.

1 Introduction

The standard model (SM) has been extremely successful in describing a wide range of phenomena in particle physics, and has survived some four decades of experimental testing. The search is underway at the Large Hadron Collider (LHC) for the only remaining undiscovered particle predicted by the SM, the Higgs boson [1–5]. A promising experimental channel for this search is the production of Higgs bosons via vector boson fusion (VBF), with subsequent decay of the Higgs bosons to τ pairs.

However, the Higgs boson in the SM suffers from quadratically divergent self-energy corrections at high energies [6]. Numerous extensions to the SM have been proposed to address these divergences. One such model, supersymmetry [7], a symmetry between fundamental bosons and fermions, results in cancellation of the divergences. The minimal supersymmetric extension to the standard model (MSSM) requires the presence of two Higgs doublets. This leads to a more complicated scalar sector, with five massive Higgs bosons: a light neutral CP-even state (h), two charged states ($H^{\pm}$), a heavy neutral CP-even state (H) and a neutral CP-odd state (A).

The mass relations among the neutral MSSM Higgs bosons are such that if $m_A \lesssim 130$ GeV, at large values of the parameter $\tan\beta$ the masses of the h and A are nearly degenerate, while that of the H is approximately 130 GeV. If $m_A \gtrsim 130$ GeV, then the masses of the A and H are nearly degenerate, while that of the h remains near 130 GeV. The precise value of the crossover point depends predominantly on the nature of the mass mixing in the top-squark states.

This Summary reports a search for the SM and the neutral MSSM Higgs bosons in pp collisions at $\sqrt{s} = 7$ TeV at the LHC, using a data sample collected in 2011 corresponding to 4.6 fb^{-1} of integrated luminosity recorded by the Compact Muon Solenoid (CMS) experiment. This search is an update to our previous search using 1.6 fb^{-1} of integrated luminosity [8] and is similar to those performed at the Tevatron [9] and by the ATLAS experiment [10] and is complementary to the MSSM Higgs search at LEP [11].

In the case of SM Higgs bosons, the gluon-fusion production of Higgs bosons has the largest cross section, but the background from Drell-Yan production of tau pairs in the mass region of interest overwhelms the expected Higgs boson signal in the $\tau\tau$ final state. To overcome this we rely on two subsamples: the VBF production of Higgs bosons, and high-p_T tau pairs from Higgs bosons produced in association with a high-p_T hadronic jet, both with decays of the Higgs boson to tau pairs. The VBF channel, with a distinct topology of two jets with a large rapidity gap, has better sensitivity due to the greatly reduced background from $Z \to \tau\tau$. Requiring a high-p_T jet greatly reduces the background from $Z \to \tau\tau$ and improves the resolution of the tau-pair invariant mass.

In the MSSM case, two main production processes contribute to $pp \to \phi + X$, where $\phi = h, H$, or A: gluon fusion through a b quark loop and direct $b\bar{b}$ annihilation from the b parton density in the beam protons. In the latter case, there is a significant probability that a b quark jet is produced centrally in association with the Higgs boson due to the enhanced $b\bar{b}\phi$ coupling if $\tan\beta$ is large. The subsample in which there is a b-tagged jet has increased sensitivity for the MSSM Higgs boson search due to the smaller relative contribution from $Z + b$.

Three independent τ pair final states where one or both taus decay leptonically are studied: $e\tau_h$, $\mu\tau_h$ and $e\mu$, where we use the symbol τ_h to indicate a reconstructed hadronic decay of a τ.

2 CMS Detector

The central feature of the CMS apparatus [12] is a superconducting solenoid, of 6 m internal diameter, providing a field of 3.8 T. Within the field volume are the silicon pixel and strip tracker, the crystal electromagnetic calorimeter and the brass/scintillator hadron calorimeter. Muons are measured in gas-ionization detectors embedded in the steel return yoke. In addition to the barrel and endcap detectors, CMS has extensive forward calorimetry.

3 Trigger and Event Selection

The triggers used to select the events for this analysis are based on the presence of electron and/or muon trigger objects [13, 14], and calorimeter deposits consistent with those expected from hadronic tau decays. As the LHC instantaneous luminosity increased, the thresholds on the p_T of the leptons and tau decay candidate increased to keep rates under control [15].

The analysis presented here makes use of particle flow techniques which combine the information from all CMS sub-detectors to identify and reconstruct individual particles in the event, namely muons, electrons, photons, and charged and neutral hadrons. The detailed description of the algorithm and its commissioning can be found elsewhere [16, 17]. The particle list is given as input to the jet, tau, and missing transverse energy ("$\not\!\!E_{\mathrm{T}}$") reconstruction. Hadronically decaying taus are reconstructed using the "HPS" algorithm [18]. Hadronic jets are reconstructed with the anti-k_T jet algorithm [19] with a cone of $\Delta R = 0.5$. The analysis here follows the same techniques as used in the earlier measurement of the production cross section for $\mathrm{Z} \to \tau\tau$ [20].

For the $\mu\tau_h$ and $\mathrm{e}\tau_h$ final states, we select events with an isolated muon with $p_{\mathrm{T}} > 15$ GeV or electron with $p_{\mathrm{T}} > 20$ GeV and $|\eta| < 2.1$, and an oppositely charged τ_h with $p_{\mathrm{T}} > 20$ GeV and $|\eta| < 2.3$. For the $\mathrm{e}\mu$ final state, we select events with an isolated electron with $|\eta| < 2.5$ and an oppositely charged isolated muon with $|\eta| < 2.1$, with $p_{\mathrm{T}} > 20$ GeV for the leading lepton and $p_{\mathrm{T}} > 10$ GeV for next-to-leading lepton. We reject events in which there are more than one e or μ.

In tau decays, due to the small invariant mass of the tau lepton, the neutrinos tend to be produced near the visible products. For W+jets decays, one of the main expected backgrounds, due the high mass of the W the neutrino should be approximately opposite the lepton and the jet misidentified as a tau, in the transverse plane. In the $\mathrm{e}\tau$ and $\mu\tau$ channels of the SM search, which focuses on lower-mass Higgs bosons (less than about 140 GeV), we require the transverse mass of the lepton and $\not\!\!E_{\mathrm{T}}$ to be less than 40 GeV in order to discriminate against the W+jets background. In the MSSM search channels, and the $\mathrm{e}\mu$ SM search channel, we use a discriminator, formed by considering the bisector of the directions of the visible tau decay products transverse to the beam direction, denoted the ζ axis [21, 22]. From the projection of the visible decay product momenta and the $\not\!\!E_{\mathrm{T}}$ vector onto the ζ axis, two values are calculated:

$$P_\zeta = p_{T,1} \cdot \zeta + p_{T,2} \cdot \zeta + \not\!\!E_{\mathrm{T}} \cdot \zeta, \tag{1}$$

$$P_\zeta^{\mathrm{vis}} = p_{T,1} \cdot \zeta + p_{T,2} \cdot \zeta \tag{2}$$

For the $\mathrm{e}\tau_h$ and $\mu\tau_h$ channels we require $P_\zeta - 0.5 P_\zeta^{\mathrm{vis}} > -20$ GeV and for the $\mathrm{e}\mu$ channel we require $P_\zeta - 0.85 P_\zeta^{\mathrm{vis}} > -25$ GeV.

To further enhance the sensitivity of the search for Higgs bosons both in the SM and in the MSSM we split the sample of selected events in several categories based on the number of

selected jets and b-tagged jets. In the SM case, we select subsamples in which there is either the jet signature of VBF, which is two jets with a wide separation in pseudorapidity, or a high-p_T jet. In the MSSM case, there is a significant probability for having a b-tagged jet in the central region, using the "track counting high efficiency" (TCHE) algorithm [23].

The SM search has three categories, which are mutually exclusive:

- ***VBF*** Requires at least two jets with $p_T > 30$ GeV, $|\Delta\eta_{jj}| > 4.0$ and $\eta_1 \cdot \eta_2 < 0$, and a dijet invariant mass $m_{jj} > 400$ GeV, with no other jet with $p_T > 30$ GeV in the rapidity region between the two jets.
- ***Boosted*** Requires one jet with $p_T > 150$ GeV, and, in the eμ channel, no b-tagged jet with $p_T > 20$ GeV.
- ***0/1 Jet*** Requires no more than one jet with $p_T > 30$ GeV, and if such a jet is present, it must have $p_T < 150$ GeV.

The MSSM search has two categories, which are mutually exclusive:

- ***b-Tag*** At most 1 jet with $p_T > 30$ GeV, at least one b-tagged jet with $p_T > 20$ GeV.
- ***No b-Tag*** At most 1 jet with $p_T > 30$ GeV, no b-tagged jet with $p_T > 20$ GeV.

The observed number of events in each channel, for the categories described above, appears in Tables 1 through 3 together with the estimated uncertainty on the yields. The largest source of events selected with these requirements comes from $Z \to \tau\tau$. We estimate the contribution from this process using an observed sample of $Z \to \mu\mu$, replacing the muons with fully simulated decays of taus. We determine the normalization for this process based on the number of observed $Z \to ee$ and $Z \to \mu\mu$ events [24]. A significant source of background arises from QCD multijet events in which there is a misidentified e or μ and a jet is misidentified as τ_h, and W+jets events in which there is a jet misidentified as a τ. The rates for these processes are estimated using the number of observed same-charge events. Other background processes include $t\bar{t}$ production and $Z \to ee/\mu\mu$ events, particularly in the eτ_h channel, due to the 2–3% probability for electrons to be misidentified as τ_h [18]. The small fake-lepton background from W+jets and QCD for the eμ channel is estimated using observed data.

The event generators PYTHIA and POWHEG are used to model the MSSM and SM Higgs boson signals, respectively, and other backgrounds. The TAUOLA [25] package is used for tau decays in all cases.

4 Tau Pair Invariant Mass Reconstruction

To distinguish the Higgs boson signal from the background, we reconstruct the tau-pair mass using a likelihood technique. The algorithm estimates the original tau three-momenta by maximizing a likelihood with respect to free parameters corresponding to the missing tau-neutrino momenta, and subject to all applicable kinematic constraints. Other terms in the likelihood take into account the tau-decay phase space and the probability density in the tau transverse momentum, parametrized as a function of the tau-pair mass. This algorithm yields a tau-pair mass with a mean consistent with the true value, and a distribution with a nearly Gaussian shape. The mass resolution is $\sim$21% at a Higgs boson mass of 130 GeV/c^2, to be compared with $\sim$24% for the (non-Gaussian) distribution of the invariant mass reconstructed from the visible tau-decay products.

Table 1: Number of expected and observed events in the event categories as described in the text for the eτ_h channel. Also given are the signal acceptances for a MSSM Higgs boson with $m_A = 120$ GeV via gluon-gluon fusion and $b\bar{b}$ annihilation and for a SM Higgs boson with $m_H = 120$ GeV produced via gluon-gluon fusion and VBF. All acceptances include the branching ratio into $\tau\tau$.

	Standard Model			MSSM	
Process	*0/1-Jet*	*Boost*	*VBF*	*Non B-Tag*	*B-Tag*
$Z \to \tau\tau$	12364 $\pm$ 856	177 $\pm$ 13	17 $\pm$ 1	13115 $\pm$ 908	126 $\pm$ 8
Fakes	6420 $\pm$ 302	27 $\pm$ 3	15 $\pm$ 2	6482 $\pm$ 305	101 $\pm$ 9
W+jets	3006 $\pm$ 220	67 $\pm$ 5	4.4 $\pm$ 0.4	5441 $\pm$ 377	32 $\pm$ 2
$Z \to ll$	5066 $\pm$ 600	27 $\pm$ 4	5 $\pm$ 1	6029 $\pm$ 646	26 $\pm$ 3
$t\bar{t}$	59 $\pm$ 6	39 $\pm$ 5	2 $\pm$ 1	44 $\pm$ 7	69 $\pm$ 10
Di-Boson	63 $\pm$ 19	5 $\pm$ 2	0.1 $\pm$ 0.1	98 $\pm$ 21	1 $\pm$ 1
Total Background	26977 $\pm$ 2004	341 $\pm$ 34	44 $\pm$ 5	31208 $\pm$ 2264	355 $\pm$ 35
$H \to \tau\tau$	48 $\pm$ 8	4.3 $\pm$ 1.1	2 $\pm$ 0.2	44 $\pm$ 4	4 $\pm$ 1
Data	27727	318	43	32062	391
Signal Efficiency					
$gg \to \phi$	-	-	-	9.17e-03	8.22e-05
$gg \to bb\phi$	-	-	-	9.75e-03	1.34e-03
$gg \to H$	8.05e-03	5.94e-04	4.50e-05	-	-
$qq \to qqH$	4.69e-03	1.42e-03	3.00e-03	-	-
$qq \to Ht\bar{t}/V$	7.06e-03	2.00e-03	2.74e-05	-	-

5 Systematic Uncertainties

Various imperfectly known or imperfectly simulated effects can alter the shape and normalization of the invariant-mass spectrum. We represent these effects via nuisance parameters in the likelihood function for the spectrum.

In the simulation we correct for the presence of multiple pp interactions in each bunch crossing ("pileup") by simulating a broad distribution of additional interactions, and then reweighting the simulated events to have the estimated distribution of additional interactions. The events in the "embedded" $Z \to \tau\tau$ sample and in other background samples obtained from data naturally contain the correct distribution of pileup interactions. In simulated samples, the modeling of the MET measurement is improved using recoil corrections derived from observed $Z \to \mu\mu$ events. Residual uncertainties in this procedure are incorporated into the systematic uncertainty values quoted below.

The main sources of normalization uncertainties include the total integrated luminosity (4.5%) [26], jet energy scale (2-5% depending on η), background normalization (Table 1- 3), Z production cross section (2.5%) [24], and lepton identification and isolation efficiency (1.0%) and trigger (1.0%). The b-tagging efficiency carries an uncertainty of 10%, and the b mistag rate is uncertain to 30%. The tau identification efficiency uncertainty is estimated to be 6% from an independent study using a tag and probe technique. In the MSSM search the uncertainty on the efficiency to identify a b jet (10%) is considered [27].

Uncertainties that contribute to mass spectrum shape variations include the tau (3%), muon (1%), and electron (1% in the barrel region, 2.5% in the endcap region) energy scale and resolution. The jet energy scale uncertainty ranges from 2.5-5%. The effect of the uncertainty in the

Table 2: Number of expected and observed events in the event categories as described in the text for the $\mu\tau_h$ channel. Also given are the signal acceptances for a MSSM Higgs boson with $m_A = 120$ GeV via gluon-gluon fusion and $b\bar{b}$ annihilation and for a SM Higgs boson with $m_H = 120$ GeV produced via gluon-gluon fusion and VBF. All acceptances include the branching ratio into $\tau\tau$.

	Standard Model			MSSM	
Process	*0/1-Jet*	*Boost*	*VBF*	*Non B-Tag*	*B-Tag*
$Z \to \tau\tau$	28115 ± 1946	294 ± 21	35 ± 2	28963 ± 2004	257 ± 18
Fakes	7852 ± 141	36 ± 2	23 ± 2	6400 ± 115	161 ± 12
W+jets	5834 ± 393	65 ± 4	9 ± 1	9571 ± 628	110 ± 7
$Z \to ll$	755 ± 95	5 ± 1	1.0 ± 0.2	900 ± 153	3 ± 1
$t\bar{t}$	143 ± 15	91 ± 12	4 ± 1	99 ± 15	147 ± 20
Di-Boson	173 ± 54	9 ± 4	0.4 ± 0.4	211 ± 45	4 ± 2
Total Background	42872 ± 2644	500 ± 46	71 ± 7	46143 ± 2961	681 ± 61
$H \to \tau\tau$	93 ± 16	6.7 ± 1.6	3 ± 0.5	83 ± 8	8 ± 1
Data	43612	500	76	47178	685
Signal Efficiency					
$gg \to \phi$	-	-	-	1.72e-02	1.72e-04
$gg \to bb\phi$	-	-	-	1.86e-02	2.45e-03
$gg \to H$	1.55e-02	8.93e-04	1.33e-04	-	-
$qq \to qqH$	8.14e-03	2.49e-03	4.97e-03	-	-
$qq \to Ht\bar{t}/V$	1.39e-02	3.16e-03	4.11e-05	-	-

Table 3: Number of expected and observed events in the event categories as described in the text for the eμ channel. Also given are the signal acceptances for a MSSM Higgs boson with $m_A = 120$ GeV via gluon-gluon fusion and $b\bar{b}$ annihilation and for a SM Higgs boson with $m_H = 120$ GeV produced via gluon-gluon fusion and VBF. The acceptances include the branching ratio into $\tau\tau$.

	Standard Model			MSSM	
Process	*0/1-Jet*	*Boost*	*VBF*	*Non B-Tag*	*B-Tag*
$Z \to \tau\tau$	11999 ± 396	99 ± 6	16 ± 2	11917 ± 393	126 ± 4
Fakes	513 ± 154	9 ± 3	2 ± 1	505 ± 151	16 ± 5
$t\bar{t}$	423 ± 32	73 ± 5	10 ± 1	161 ± 12	283 ± 21
Di-Boson	586 ± 88	21 ± 3	2 ± 0.4	542 ± 81	56 ± 8
Total Background	13008 ± 435	193 ± 9	29 ± 2	12619 ± 429	465 ± 23
$H \to \tau\tau$ (SM)	37 ± 1	2 ± 0.2	1 ± 0.1	37 ± 1	1 ± 0.1
Data	13372	191	27	12978	472
Signal Efficiency					
$gg \to \phi$	-	-	-	3.19e-02	4.61e-04
$bb \to \phi$	-	-	-	2.88e-02	4.84e-03
$gg \to H$	6.39e-03	1.84e-04	3.00e-05	-	-
$qq \to H$	3.10e-03	8.09e-04	1.97e-03	-	-
$qq \to t\bar{t}/VH$	3.87e-03	6.85e-04	2.00e-06	-	-

$\not\!\!E_T$ scale, mainly due to pileup effects, is incoporated by varying the mass spectrum shape as described below.

In the SM search theoretical uncertainties on the Higgs production are included (12% for ggH and 3.5% for qqH) [28].

6 Likelihood Fit

To search for the presence of a Higgs boson signal in the selected events, we perform a binned maximum likelihood fit to the tau-pair invariant-mass spectrum, $m_{\tau\tau}$.

Systematic uncertainties are represented by nuisance parameters, which we remove by marginalization, assuming a log normal prior for normalization parameters, and Gaussian priors for mass-spectrum shape uncertainties. The uncertainties that affect the shape of the mass spectrum, mainly those corresponding to the energy scales, are represented by nuisance parameters whose variation results in a continuous modification of the spectrum shape [29].

The parameter representing the tau identification uncertainty affects taus from the Higgs boson signal and the main background, $Z \to \tau\tau$, equally. This effectively allows the observed $Z \to \tau\tau$ events to provide an *in situ* calibration of this efficiency, except for Higgs boson masses near that of the Z.

7 Results

Figures 1 and 2 show the distributions of the tau-pair mass $m_{\tau\tau}$ summed over the three search channels, for each category, compared with the background prediction.

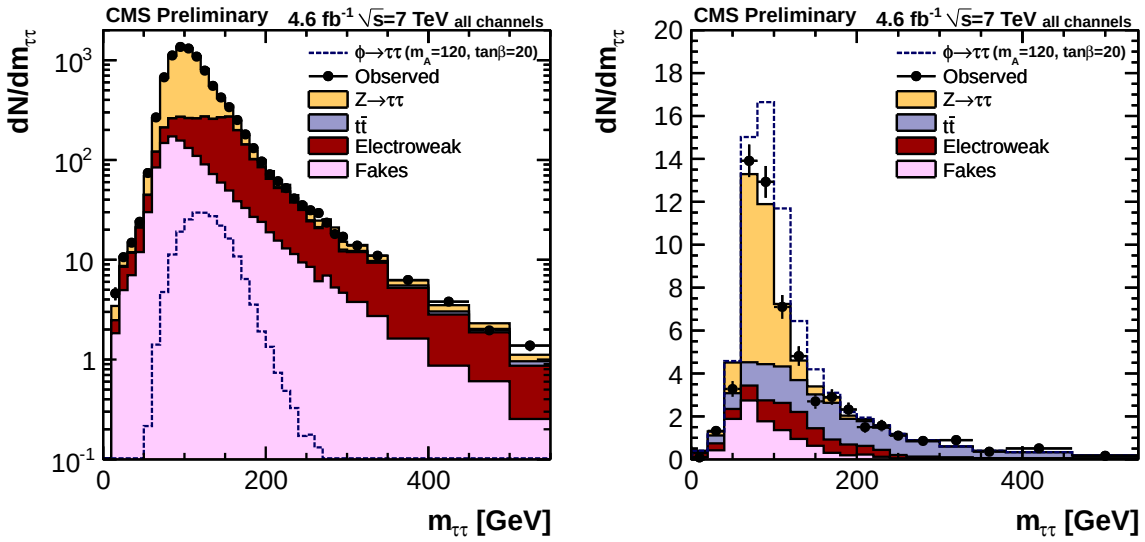

Figure 1: Tau-pair invariant mass, $m_{\tau\tau}$, in the MSSM Higgs boson search categories: No b-Tag category (left), b-Tag (right).

The invariant mass spectra for both the MSSM and SM categories show no evidence for the presence of a Higgs boson signal, and we set 95% CL (confidence level) upper bounds on the Higgs boson cross section times the tau-pair branching fraction (denoted by $\sigma_\phi \cdot B_{\tau\tau}$) in each case.

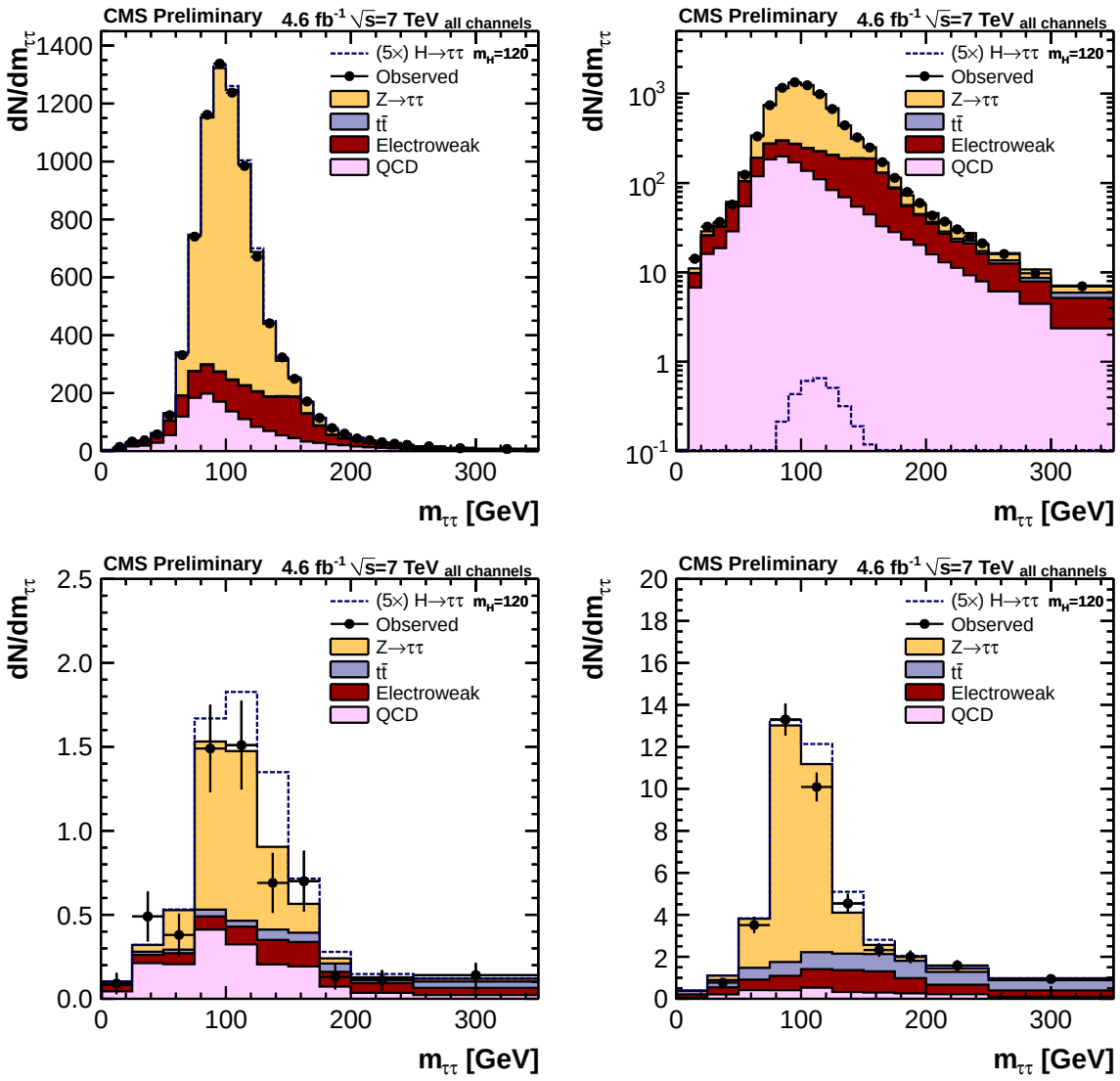

Figure 2: Tau-pair invariant mass, $m_{\tau\tau}$, in the SM Higgs boson search categories: 0/1 Jet (top row, linear and log vertical scale), VBF (lower left), and Boosted (lower right).

7.1 MSSM Limits

Figure 3 shows the upper bound on $\sigma_\phi \cdot B_{\tau\tau}$ as a function of m_A, where we use as the signal acceptance model the combined visible mass spectra from the gg and $b\bar{b}$ production processes for h, A, and H, and assuming $\tan\beta = 30$ [28]. The plot also shows the one- and two-standard-deviation range of expected upper limits for various potential experimental outcomes. The observed limits are well within the expected range assuming no signal. The observed and expected upper limits are shown in Tab. 4.

We can interpret the upper limits on $\sigma_\phi \cdot B_{\tau\tau}$ in the MSSM parameter space of $\tan\beta$ versus m_A for an example scenario. We use here the m_h^{max} [30, 31] benchmark scenario in which $M_{\text{SUSY}} = 1$ TeV; $X_t = 2M_{\text{SUSY}}$; $\mu = 200$ GeV; $M_{\tilde{g}} = 800$ GeV; $M_2 = 200$ GeV; and $A_b = A_t$, where M_{SUSY} denotes the common soft-SUSY-breaking squark mass of the third generation; $X_t = A_t - \mu/\tan\beta$ the stop mixing parameter; A_t and A_b the stop and sbottom trilinear couplings, respectively; μ the Higgsino mass parameter; $M_{\tilde{g}}$ the gluino mass; and M_2 the SU(2)-gaugino mass parameter.

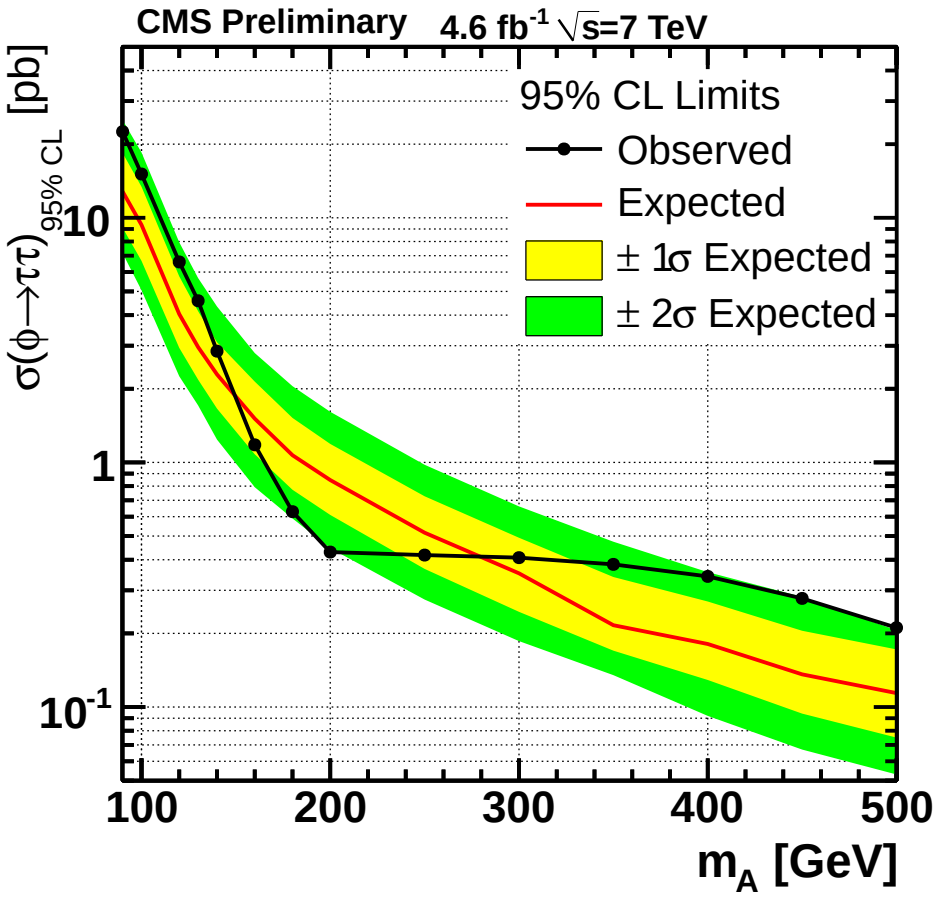

Figure 3: The expected one- and two-standard-deviation ranges and the observed 95% CL upper limits on $\sigma_\phi \cdot B_{\tau\tau}$ as a function of m_A. The signal acceptance is based on the MSSM model described in the text, assuming $\tan\beta = 30$.

Table 4: Expected range and observed 95% CL upper limits for $\sigma_\phi \cdot B_{\tau\tau}$ as functions of m_A, for the MSSM search, and 95% CL upper bound on $\tan\beta$ in the $m_h^{\max}$ scenario described in the text.

MSSM Higgs	Expected Limit [pb]						
m_A	-2σ	-1σ	Median	$+1\sigma$	$+2\sigma$	Obs. Limit [pb]	$\tan\beta$
90 GeV	7.16	9.1	12.8	18.4	25.1	22.5	10.8
100 GeV	5.06	6.67	9.36	13.4	18.5	15.1	10.9
120 GeV	2.25	2.94	4.04	5.76	7.94	6.6	10.6
130 GeV	1.71	2.18	2.96	4.15	5.67	4.58	8.4
140 GeV	1.24	1.66	2.29	3.1	4.34	2.85	9.4
160 GeV	0.79	1.08	1.51	2.14	2.8	1.18	7.8
180 GeV	0.59	0.77	1.07	1.52	2.05	0.63	7.4
200 GeV	0.45	0.61	0.85	1.19	1.61	0.43	7.8
250 GeV	0.28	0.37	0.52	0.73	0.98	0.42	12.6
300 GeV	0.19	0.25	0.35	0.49	0.66	0.41	19.2
350 GeV	0.14	0.17	0.22	0.34	0.47	0.38	27.4
400 GeV	0.092	0.13	0.18	0.27	0.36	0.34	35.4
450 GeV	0.067	0.094	0.14	0.21	0.28	0.28	42.6
500 GeV	0.053	0.075	0.11	0.17	0.21	0.21	49.7

The value of M_1 is fixed via the GUT relation $M_1 = (5/3)M_2 \sin\theta_W / \cos\theta_W$. In determining these bounds on $\tan\beta$, shown in Table 4 and in Fig. 4, we have used the central values of the Higgs boson cross sections as a function of $\tan\beta$ reported by the LHC Higgs Cross Section Working Group [28]. The cross sections have been obtained from the GGH@NNLO [32, 33] and HIGLU [34] programs for the gluon-fusion process. For the $b\bar{b} \to \phi$ process, the 4-flavor calculation [35, 36] and the 5-flavor calculation as implemented in the BBH@NNLO [37] program have been combined using the Santander scheme [38]. Rescaling of the corresponding Yukawa couplings by the MSSM factors calculated with FeynHiggs [39] has been applied.

The present results exclude a region in $\tan\beta$ down to values smaller than those excluded by the Tevatron experiments [9] for $m_A \lesssim 140$ GeV/c^2, and significantly extend the excluded region of MSSM parameter space at larger values of m_A. Figure 4 also shows the region excluded by the LEP experiments [11].

7.2 SM Limits

In the VBF and boosted categories the mass spectra show no evidence for the presence of a Higgs boson signal. We set a 95% CL upper limit on the ratio of the cross section times branching ratio to the nominal SM Higgs cross section. Figure 5 shows the observed and the mean expected 95% CL upper limits for Higgs mass hypothesis ranging from 110 to 145 GeV/c^2. The bands represent the 1 σ and 2 σ probability intervals around the expected limit. Table 5 shows the result for selected mass values. We set an upper limit on $\sigma_H \cdot B_{\tau\tau}$ in the range 2.8-6.3 times the SM value.

8 Conclusion

In conclusion, we have performed a search for neutral MSSM and SM Higgs bosons, using a sample of CMS data from proton-proton collisions at a center-of-mass energy of 7 TeV at the LHC, corresponding to an integrated luminosity of 4.6 fb^{-1}. The tau-pair decay mode in final states with one e or μ plus a hadronic decay of a tau and the eμ final state are used, and split

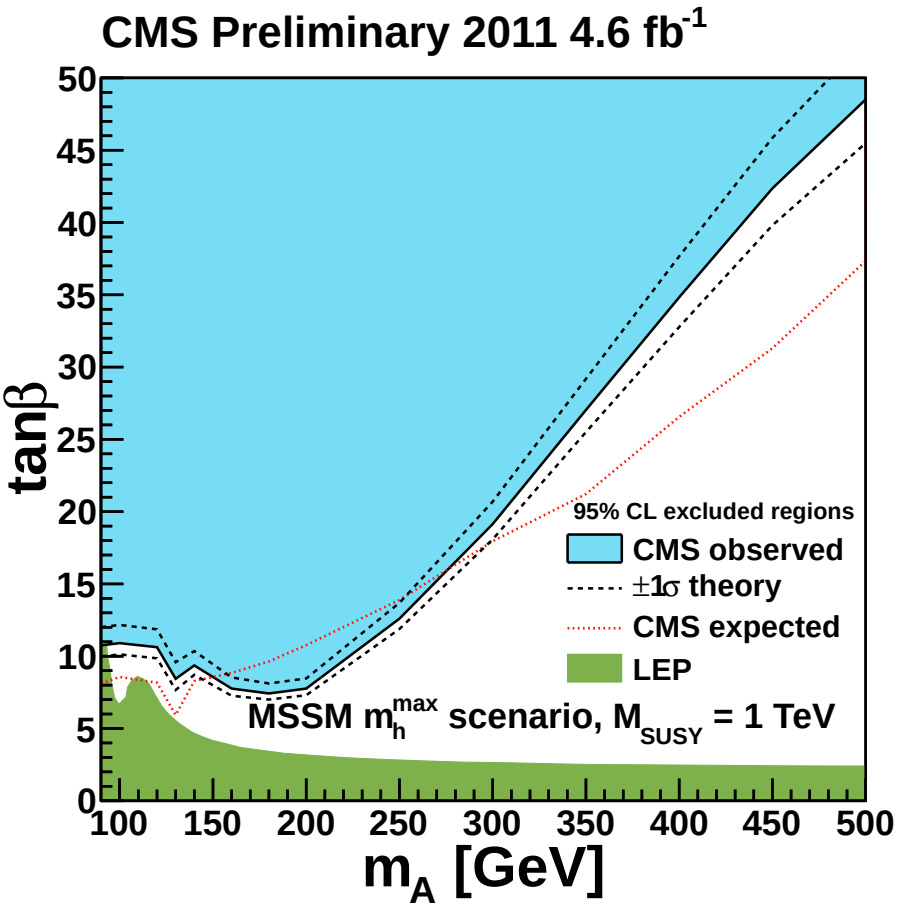

Figure 4: Region in the parameter space of $\tan\beta$ versus m_A excluded at 95% CL in the context of the MSSM $m_h^{\max}$ scenario, with the effect of $\pm 1\sigma$ theoretical uncertainties shown.

Table 5: Expected range and observed 95% CL upper limits on the cross section normalized to the SM expectation as functions of m_H, for the SM search.

SM Higgs	Expected Limit [over σ(SM)]					
m_H	-2σ	-1σ	Median	$+1\sigma$	$+2\sigma$	Obs. Limit [pb]
110 GeV	1.44	1.83	2.56	3.73	5.29	3.48
115 GeV	1.25	1.54	2.19	3.13	4.42	2.86
120 GeV	1.22	1.61	2.27	3.33	4.73	3.15
125 GeV	1.37	1.72	2.34	3.39	4.75	3.55
130 GeV	1.46	1.94	2.63	3.79	5.34	4.03
135 GeV	1.86	2.37	3.28	4.7	6.58	4.55
140 GeV	1.94	2.6	3.59	5.19	6.99	4.89
145 GeV	2.7	3.41	4.77	6.89	9.35	6.28

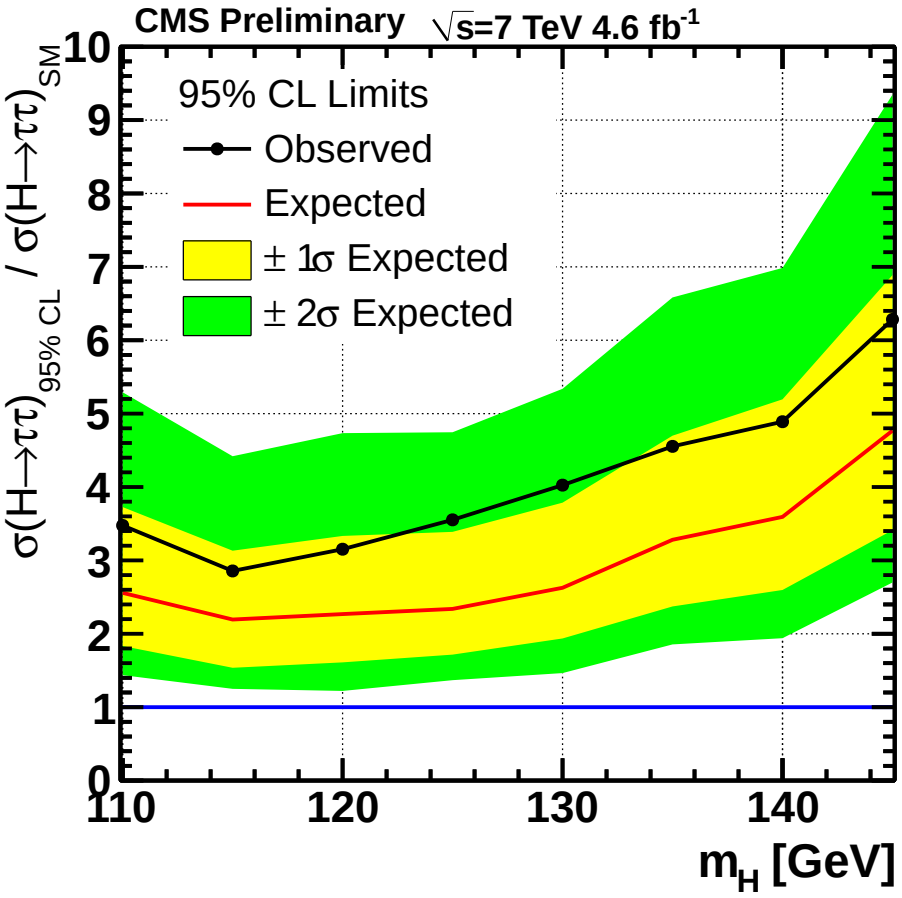

Figure 5: The expected one- and two-standard-deviation ranges and the observed 95% CL upper limits on the cross section normalized to the SM expectation as a function of m_H.

into final states with b-tagged jets for the MSSM search, forward jets from VBF for the SM search or high-p_T tau pairs for the SM search. In the MSSM case the observed tau-pair mass spectrum reveals no evidence for neutral Higgs boson production, and we determine an upper bound on the product of the Higgs boson cross section and tau-pair branching fraction as a function of m_A. These results, interpreted in the MSSM parameter space of $\tan\beta$ versus m_A, in the m_h^{max} scenario, exclude a previously unexplored region reaching as low as $\tan\beta = 7.8$ at $m_A = 160$ GeV. In the SM case the statistical level is low, and the observed and predicted mass spectra can be incorporated into combined multi-channel searches for the SM Higgs boson. We set an upper limit on $\sigma_H \cdot B_{\tau\tau}$ of 2.8 times the SM value at $m_H = 115$ GeV.

References

[1] P. W. Higgs, "Broken Symmetries, Massless Particles and Gauge Fields", *Phys. Lett.* **12** (1964) 132. doi:10.1016/0031-9163(64)91136-9.

[2] P. W. Higgs, "Broken Symmetries and the Masses of Gauge Bosons", *Phys. Rev. Lett.* **13** (1964) 508. doi:10.1103/PhysRevLett.13.508.

[3] F. Englert and R. Brout, "Broken Symmetry and the Mass of Gauge Vector Mesons", *Phys. Rev. Lett.* **13** (1964) 321. doi:10.1103/PhysRevLett.13.321.

[4] G. Guralnik, C. Hagen, and T. Kibble, "Global Conservation Laws and Massless Particles", *Phys. Rev. Lett.* **13** (1964) 585. doi:10.1103/PhysRevLett.13.585.

[5] P. W. Higgs, "Spontaneous Symmetry Breakdown without Massless Bosons", *Phys. Rev.* **145** (1966) 1156. doi:10.1103/PhysRev.145.1156.

[6] E. Witten, "Mass Hierarchies in Supersymmetric Theories", *Phys. Lett. B* **105** (1981) 267. doi:10.1016/0370-2693(81)90885-6.

[7] S. P. Martin, "A Supersymmetry Primer", (1997). arXiv:hep-ph/9709356. See also references therein.

[8] CMS Collaboration, "Search for Neutral Higgs Bosons Decaying to Tau Pairs in pp Collisions at $\sqrt{s}$=7 TeV", *CMS Physics Analysis Summary* **CMS-PAS-HIG-11-020** (2011).

[9] CDF and D0 Collaboration, "Combined CDF and D0 Upper Limits on MSSM Higgs Boson Production in Tau-Tau Final States with up to 2.2 fb^{-1}", arXiv:1003.3363.

[10] ATLAS Collaboration, "Search for neutral MSSM Higgs Bosons Decaying to $\tau^+\tau^-$ Pairs in Proton-Proton Collisions at $\sqrt{s}$ = 7 TeV with the ATLAS Experiment", **ATLAS-CONF-2011-024** (2011).

[11] LEP Higgs Working Group, "Search for Neutral MSSM Higgs Bosons at LEP", *Eur. Phys. J.* **C47** (2006) 547–587. doi:10.1140/epjc/s2006-02569-7.

[12] CMS Collaboration, "The CMS Experiment at the CERN LHC", *JINST* **0803** (2008) S08004. doi:10.1088/1748-0221/3/08/S08004.

[13] CMS Collaboration, "Electron Reconstruction and Identification at $\sqrt{s} = 7$ TeV", *CMS Physics Analysis Summary* **CMS-PAS-EGM-10-004** (2010).

[14] CMS Collaboration, "Performance of muon identification in pp collisions at $\sqrt{s}$ = 7 TeV", *CMS Physics Analysis Summary* **CMS-PAS-MUO-10-002** (2010).

[15] CMS Collaboration, "Commissioning of the particle-flow event reconstruction with leptons from J/Psi and W decays at 7 TeV", *CMS Physics Analysis Summary* **CMS-PAS-PFT-10-003** (2010).

[16] CMS Collaboration, "Particle–Flow Event Reconstruction in CMS and Performance for Jets, Taus, and $E_{\mathrm{T}}^{\mathrm{miss}}$", *CMS Physics Analysis Summary* **CMS-PAS-PFT-09-001** (2009).

[17] CMS Collaboration, "Commissioning of the Particle-Flow Reconstruction in Minimum-Bias and Jet Events from pp Collisions at 7 TeV", *CMS Physics Analysis Summary* **CMS-PAS-PFT-10-002** (2010).

[18] CMS Collaboration, "Performance of tau lepton reconstruction and identification in CMS", *to appear in JINST* (2011) arXiv:hep-ex/1109.6034.

[19] M. Cacciari, G. P. Salam, and G. Soyez, "The anti-k_T jet clustering algorithm", *JHEP* **04** (2008) 063, arXiv:0802.1189. doi:10.1088/1126-6708/2008/04/063.

[20] CMS Collaboration, "Measurement of Inclusive $Z \to \tau\tau$ Cross Section in pp Collisions at $\sqrt{s}$=7 TeV", *JHEP* **2011** (2011) 117. doi:10.1007/JHEP08(2011)117.

[21] CDF Collaboration, "Search for MSSM Higgs Decaying to Tau Pairs", *CDF Public Note* **7161** (2004).

[22] C.C.Almenar, "Search for the neutral MSSM Higgs bosons in the tau tau decay channels at CDF Run II", *PhD Thesis* (2008).

[23] CMS Collaboration, "Commissioning of b-jet identification with pp collisions at $\sqrt{s}$ = 7 TeV", *CMS Physics Analysis Summary* **CMS-PAS-BTV-10-001** (2010).

[24] CMS Collaboration, "Measurement of Inclusive W and Z Cross Sections in pp Collisions $\sqrt{s}$=7 TeV", *JHEP* **1101** (2011) 080. doi:10.1007/JHEP01(2011)080.

[25] Z. Wąs et al., "TAUOLA the Library for Tau Lepton Decay", *Nucl. Phys. B, Proc. Suppl.* **98** (2001) 96. doi:10.1016/S0920-5632(01)01200-2.

[26] CMS Collaboration, "Measurement of CMS Luminosity", *CMS Physics Analysis Summary* **EWK-10-004** (2010).

[27] CMS Collaboration, "Performance of b-jet identification in CMS", *CMS Physics Analysis Summary* **CMS-PAS-BTV-11-001** (2011).

[28] LHC Higgs Cross Section Working Group, S. Dittmaier, C. Mariotti et al., "Handbook of LHC Higgs Cross Sections: Inclusive Observables", arXiv:1101.0593.

[29] J. S. Conway, "Nuisance Parameters in Likelihoods for Multisource Spectra", *submitted to Proceedings of PhyStat 2011* (2011) arXiv:1103.0354.

[30] M. S. Carena et al., "Suggestions for Benchmark Scenarios for MSSM Higgs Boson Searches at Hadron Colliders", *Eur. Phys. J.* **C26** (2003) 601–607. doi:10.1140/epjc/s2002-01084-3.

[31] M. S. Carena et al., "MSSM Higgs Boson Searches at the Tevatron and the LHC: Impact of Different Benchmark Scenarios", *Eur. Phys. J.* **C45** (2006) 797–814. doi:10.1140/epjc/s2005-02470-y.

[32] R. V. Harlander and W. B. Kilgore, "Next-to-next-to-leading order Higgs production at hadron colliders", *Phys. Rev. Lett.* **88** (2002) 201801. doi:10.1103/PhysRevLett.88.201801.

[33] R. V. Harlander and W. B. Kilgore, "Production of a pseudo-scalar Higgs boson at hadron colliders at next-to-next-to leading order", *JHEP* **10** (2002) 017. doi:10.1088/1126-6708/2002/10/017.

[34] M. Spira, "HIGLU: A Program for the Calculation of the Total Higgs Production Cross Section at Hadron Colliders via Gluon Fusion including QCD Corrections", arXiv:hep-ph/9510347.

[35] S. Dittmaier, M. Kramer, and M. Spira, "Higgs radiation off bottom quarks at the Tevatron and the LHC", *Phys. Rev.* **D70** (2004) 074010. doi:10.1103/PhysRevD.70.074010.

[36] S. Dawson, C. Jackson, L. Reina et al., "Exclusive Higgs boson production with bottom quarks at hadron colliders", *Phys. Rev.* **D69** (2004) 074027, arXiv:hep-ph/0311067. doi:10.1103/PhysRevD.69.074027.

[37] R. V. Harlander and W. B. Kilgore, "Higgs boson production in bottom quark fusion at next-to- next-to-leading order", *Phys. Rev.* **D68** (2003) 013001. doi:10.1103/PhysRevD.68.013001.

[38] R. Harlander, M. Kramer, and M. Schumacher, "Bottom-quark associated Higgs-boson production: reconciling the four- and five-flavour scheme approach", **CERN-PH-TH/2011-134 - FR-PHENO-2011-009 - TTK-11-17 - WUB/11-04** (2011).

[39] S. Heinemeyer, W. Hollik, and G. Weiglein, "FeynHiggs: a program for the calculation of the masses of the neutral CP-even Higgs bosons in the MSSM", *Comput. Phys. Commun.* **124** (2000) 76–89. doi:10.1016/S0010-4655(99)00364-1.